Retention Behavior of Linear and Ring Polystyrene at the Chromatographic Critical Condition

Wonmok Lee, Hyunjung Lee, Hee Cheong Lee, Donghyun Cho, and Taihyun Chang*

Department of Chemistry and Polymer Research Institute, Pohang University of Science and Technology, Pohang, 790-784, Korea

Alexei A. Gorbunov*

State Institute for Highly Pure Biopreparations, 197110 St. Petersburg, Russia

Jacques Roovers

Institute for Chemical Process and Environmental Technology, National Research Council of Canada, Ottawa, Ontario, Canada K1A 0R9

Received May 29, 2001; Revised Manuscript Received October 2, 2001

ABSTRACT: Chromatographic retention of linear and ring polystyrene was investigated near the chromatographic critical condition. Reversed phase silica columns of four different pore sizes were employed to examine the pore size dependence. Adjusting the column temperature, the critical condition for linear polystyrene was searched for each column with a mixed mobile phase of CH_2Cl_2/CH_3CN (57/43 v/v). It was practically impossible to establish an unambiguous critical condition with a single pore size column for a wide molecular weight range of polystyrenes, in particular with narrow pore size columns. At the best available condition, retentions of nine different molecular weight ring polystyrenes were measured relative to their linear precursors for each pore-sized column. As predicted theoretically, the partition coefficient (K) of ring polymers vs the size ratio of polymer chain to pore (R/d) shows a good linear relationship in the large pore regime ($R/d \ll 1$). This linearity is found to be universal for all the pore sizes, which is consistent with the theoretical prediction. However, the K vs R/d dependency at the large pore regime did not follow the theoretical prediction quantitatively. In the narrow-pore regime ($R/d \gg 1$) the experimental results did not follow the theory for ideal-chain ring macromolecules even qualitatively. To explain the observed chromatographic behavior at $R/d \gg 1$, the scaling theory accounting for the polymer excluded volume was used, and the definition of the critical condition was revised. This analysis gave some keys for understanding the results at $R/d \gg 1$ and revealed the possible nonequivalence of the conditions for theory and experiment as the most probable reason for observed discrepancies.

Introduction

Study on the synthesis and physical properties of ring polymers has attracted considerable interest. Because of its topological peculiarity, they show distinct properties compared to linear polymers, and various physical properties of ring polymers have been predicted theoretically as well as by computer simulation studies.[1−3] Those predictions were also examined by a variety of experimental studies such as viscometry,[4−7] neutron scattering,[7−10] light scattering,[4,5,10,11] viscoelastic property,[12,13] liquid chromatography,[14−17] and MALDI-TOF mass spectrometry.[17−19]

To obtain high molecular weight ring polymers with narrow molecular weight distribution, anionic polymerization has been most often employed. The basic strategy is to form precursor polymers with two carbanion end groups and to have them react intramolecularly, under extreme dilution, with a difunctional electrophile to close the ring.[4,14,20−23] However, side reactions produce linear precursor polymers, and intermolecular reactions simultaneously produce dimeric and higher molecular weight linear polymers, which makes fractionation necessary to obtain ring polymers with high purity. For the fractionation of ring polymers from a ring-closure reaction mixture, two methods have been employed most often: fractional precipitation[4,5,7,14,21−25] and preparative size exclusion chromatography (SEC).[26,27] However, none of the methods have been fully successful in separating the ring polymers from the side products. The SEC retention times (hydrodynamic volume of polymer chains) of a ring polymer and its linear precursor are not sufficiently different to allow complete resolution of the elution peaks. The ultracentrifugation sedimentation method was reported to be more successful in distinguishing rings from the linear precursor by Roovers et al., but it is not suitable for preparative purposes.[14,23]

Recently, Blagodatskikh and Gorshkov,[28] Lee et al.,[16] and Lepoittevin et al.[17] reported that ring polymers could be efficiently separated from their linear precursors by liquid chromatography at the critical condition (LCCC). The critical condition is usually defined as a point at which the weak attractive enthalpic interaction effect is exactly compensated by the entropic exclusion effect for a linear homopolymer, and the polymer species elutes near the retention time of the injection solvent independent of its molecular weight.[29] LCCC has been efficiently employed to characterize polymer blends, block copolymers, telechelic polymers, etc.[30−34] The

* Corresponding authors. Taihyun Chang: TEL +82-54-279-2109; FAX +82-54-279-3399; E-mail tc@postech.ac.kr. Alexei A. Gorbunov: TEL +7-812-2307863; FAX +7-812-2304948; E-mail zero@aag.usr.hpb.spb.ru.

10.1021/ma0109222 CCC: $22.00
Published on Web 12/18/2001

LCCC separation of linear and ring polymers is based on the theoretical development of Gorbunov and Skvortsov which described a chromatographic retention behavior of polymers of these types under the critical conditions.[35] The available experimental results are in qualitative agreement with the theoretical prediction.[16,17,28] In this study, we extend the previous LCCC study[16] with a variety of pore-sized columns and more systematically compared the experimental result with the theory.

Theory

Theory of LCCC for Ideal-Chain Linear and Ring Macromolecules. The analytical theory of LCCC of ideal-chain linear and ring polymers is based on the same model as the well-known Casassa theory of size-exclusion chromatography,[36] but additionally takes into account the weak attractive forces between polymer chain segments and pore walls, corresponding to the LCCC conditions. The mathematical formulation is based on the diffusion equation for an ideal flexible polymer chain of N statistical segments (each segment of the size b):

$$\frac{\partial}{\partial N} P - \frac{b^2}{6} \nabla^2 P = 0 \tag{1}$$

where $P(N,\vec{r}_1,\vec{r}_2)$ is the distribution function of a chain with ends at points $\vec{r}_1$ and $\vec{r}_2$ of the in-pore space. The solution of eq 1 without space restriction expresses P in the well-known form of the Gaussian distribution function and gives $R \equiv R_{lin} = b(N/6)^{1/2}$ for the radius of gyration of an unconfined linear ideal chain and $R_{ring} = R/\sqrt{2}$ for an unconfined ideal-ring macromolecule under the constraint of $\vec{r}_1 = \vec{r}_2$.

In the Casassa theory of size-exclusion chromatography the repulsive-wall boundary condition has been used:

$$P|_{wall} = 0 \tag{2}$$

The LCCC situation is described by a different boundary condition:

$$\left.\frac{\partial P}{\partial \vec{r}}\right|_{wall} = 0 \tag{3}$$

This boundary condition was first introduced by de Gennes[37] to describe the behavior of a polymer chain at the adsorption−desorption transition point where the entropy and enthalpy effects for an infinitely long polymer chain interacting with a surface are mutually compensated. The solution of eq 1 under the appropriate boundary condition leads to the exact analytical expressions for the equilibrium distribution coefficients of linear (K_{lin}) and ring (K_{ring}) macromolecules between the interstitial and the pore space by integration of the sub-partition function P over all in-pore space of volume. For a slitlike pore of width $2d$ the result for the distribution coefficient of the ideal linear chain at the adsorption transition point is very simple: K_{lin} does not depend on chain length N or pore size d (for the ideal-chain model the same is true for any other pore geometry).

$$K_{lin} = 1 \tag{4}$$

In contrast, the distribution coefficient of the ring macromolecule K_{ring} at the same critical conditions happens to be dependent on both N and d being a function of a dimensionless molecule-to-pore size ratio $g = R/d$ (R is the radius of gyration of an unconfined linear chain). The ideal-chain theoretical expression for K_{ring} at the critical conditions has the form[35,38]

$$K_{ring} = \sqrt{\pi} g \sum_{k=0}^{\infty} \exp\left[-\left(\frac{k\pi}{2} g\right)^2\right] \tag{5}$$

This exact but complicated function can be reasonably approximated by two asymptotes corresponding to small and large values of the molecule-to-pore size ratio.

$$\text{at } R/d \ll 1: \quad K_{ring} = 1 + \frac{\sqrt{\pi}}{2}\frac{R}{d} \tag{6}$$

$$\text{at } R/d \gg 1: \quad K_{ring} = \sqrt{\pi}\frac{R}{d} \tag{7}$$

Chromatographic Behavior in Wide Pores: General Features. The result for the distribution coefficient of a ring polymer chain in the wide-pore regime, eq 6, can be presented in a more general form:

$$K_{ring} = 1 + \frac{s}{2}\Sigma \tag{8}$$

The parameter s in eq 8 is the chromatographic diameter of a macromolecule that is equal to the average span of a polymer chain (a maximum projection of a chain over an axis[39]). For an ideal cyclic chain, $s = \sqrt{\pi}R = \sqrt{2\pi}R_{ring}$ is proportional to $M^{0.5}$. In a thermodynamically good solvent, s should be proportional to M^{α} with $0.5 < \alpha < 0.6$. The parameter Σ is a specific surface of the porous stationary phase defined as the ratio of the total surface area of all pores S_p to their total volume V_p. For pores of regular shape, the parameter Σ is inversely proportional to the characteristic pore size: $\Sigma = p/d$, where p is an index related to pore geometry ($p = 1$, 2, and 3 for slitlike, cylindrical, and spherical pores, respectively). Unlike the model-dependent parameter d, the parameter Σ is meaningful even in the case of adsorbents with pores of irregular shape as well as for polydisperse porous media.[40]

Scaling Theory for Linear and Ring Macromolecules with Excluded Volume in Narrow Pores. The behavior of linear and ring polymers in narrow pores is not so simple and universal as in wide pores. To describe this behavior, the scaling theory has been developed by Skvortsov and Gorbunov.[38,41] As follows from this theory, both pore geometry and polymer chain excluded-volume effects can significantly influence the behavior of polymers at $R/d \gg 1$ at the chromatographic critical condition.

The distribution coefficients of linear and ring macromolecules at $R/d \gg 1$ at the point of exclusion−adsorption transition point should follow the common scaling form[38,41]

$$K \propto \left(\frac{R}{d}\right)^{\delta} \tag{9}$$

with the index δ depending on the polymer chain topology, pore geometry, and the solvent quality. The

scaling theory gives the following expressions for δ_{lin} and δ_{ring}:

$$\delta_{lin} = \frac{\gamma_f - \gamma_3}{\nu_3} \tag{10}$$

$$\delta_{ring} = 3 - f\frac{\nu_f}{\nu_3} \tag{11}$$

where $f = 3 - p$ is a pore dimensionality index ($f = 1$ for cylinder and 2 for slit), ν_f is the scaling index for the f-dimensional chain radius $R_f \propto M^{\nu_f}$, and γ is another scaling index, dependent on the space dimensions[42] (for ideal chains $\gamma_f = 1$, for self-avoiding random walks $\gamma_3 = {}^7/_6$, $\gamma_2 = {}^4/_3$, and $\gamma_1 = 1$). For the ideal-chain and slitlike pore model $f = 2$, $\gamma_3 = \gamma_2 = 1$, $\nu_3 = \nu_2 = {}^1/_2$, the scaling theory gives qualitatively the same results (K_{lin} = constant, $K_{ring} \propto R/d$) as those given by eqs 4 and 7 of the analytical theory.

On the other hand, in the case of macromolecules with excluded volume the scaling theory predicts different scaling laws at $R/d \gg 1$, which depend on both pore geometry and solvent quality. For example, in the case of the thermodynamically good solvent and the slitlike pore ($\nu_3 = {}^3/_5$, $\nu_2 = {}^3/_4$), eqs 9 and 11 give the scaling result $K_{ring} \propto (R/d)^{1/2}$, which is considerably different from that of the ideal-chain theory.

Critical Condition: A New More General Definition. The theory for the ring macromolecules at the critical point reveals one interesting fact concerning the definition of the critical condition. Usually the condition for critical interaction is defined as a point (in the experiment this is usually a certain temperature at specific mobile and stationary phases) at which the distribution coefficient becomes independent of molecular weight. This definition is fully consistent with the theoretical result for the ideal linear chain (eq 4). On the other hand, eqs 5−7 obtained for ring macromolecules under the same conditions appear to be in conflict with this definition. The reason is in the inconsistency of the above definition. In fact, the only physically meaningful definition of the critical point is the definition, which is based on the consideration of the adsorption−exclusion transition that takes place with macromolecules interacting with the pores of chromatographic columns.[38] For an infinitely long macromolecule this transition occurs when the increasing attractive interaction between the polymer segments and the pore walls reaches some critical level. The most general and unambiguous definition of the critical point is related to the transition properties of the asymptotically long polymer chain of N segments: at the transition point the change of the free energy per one segment, $\Delta F/N \propto (-\ln K)/N$ must vanish at $N \to \infty$. It can be easily shown that both critical condition expressions, eqs 4 and 7, for K of linear and ring macromolecules satisfy this general definition. In fact, the general definition of the critical condition is equivalent to the statement that at the critical point there must not be factors in the expression for K, which would be *exponentially* increasing or decreasing function of N. Any (even very small) deviation from the critical condition leads to the appearance of such exponential factors, which become significant at high N and dominant at very high N.

The scaling theory for linear macromolecules also revealed an interesting result: the distribution coefficient of a linear polymer with excluded volume in the critical condition may also depend on R! One can easily verify this by putting, for example, into eqs 9 and 10 the values $f = 2$, $\nu_3 = {}^3/_5$, $\gamma_3 = {}^7/_6$, and $\gamma_2 = {}^4/_3$ (good solvent, slitlike pore)—the result will be $K_{lin} \propto (R/d)^{5/18}$. Like the critical condition results for the ring polymer, this result for linear polymer looks very strange from the standpoint of the traditional definition of the critical condition (independence on N), but without any problems it satisfies the above-discussed general definition of the critical condition.

Unfortunately, it is difficult to use the general definition of the critical condition in practice, since it requires chromatographic measurements at very high molecular weight. It is well-known that the chromatographic data for very long polymers near the critical condition are poorly reproducible: even small instabilities in the interaction energy would lead to dramatic changes in the distribution coefficient.

Table 1. Molecular Characteristics of Ring PSs Used

sample code	M_w (kg/mol)	M_w/M_n[b]	sample code	M_w (kg/mol)	M_w/M_n[b]
R17	4.7 (4.6)[a]	1.09	R8	64.0	1.08
R7	11.8	1.07	R9	75.1	1.04
R16	16.8 (15.8)[a]	1.03	R18	148	1.03
R1	23.3 (21.8)[a]	1.05	R10	170	1.04
R4	46.6	1.07			

[a] Values in parentheses are MALDI-TOF MS results. [b] Measured by SEC for the ring polymers before LCCC fractionation.

Experimental Section

Materials. Nine ring polystyrene (PS) samples in the molecular weight range from 5 to 200 kg/mol were used as listed in Table 1. The polymerization and fractionation scheme as well as characterization results were reported previously.[5,23] Including the previous characterization by us,[16] it has been generally assumed that the molecular weights of linear precursors and ring polymers are identical. However, we found that the molecular weights of ring polymers were not exactly the same as the linear precursors likely due to the fractionation procedure after the cyclization reaction to remove the unreacted linear precursors.[19] Therefore, we examined the molecular weights more carefully by size exclusion chromatography (SEC) coupled with a multiangle laser light scattering detector (MALLS, Wyatt, Mini-DAWN) and a refractive index detector (Wyatt, OptiLab). Two mixed bed columns (Polymer Lab., Mixed-C, 300 × 7.8 mm i.d.) and tetrahydrofuran (THF, Aldrich, HPLC grade) were used as stationary and mobile phase, respectively. The column temperature was maintained at 40 °C using a column oven (Eppendorf, TC-50). To compare the molecular weight of the sample more precisely, MALDI-TOF MS (Bruker, Reflex-III) experiments were performed for three low molecular weight samples. The matrix was dithranol (Aldrich), and the cation was silver.

LCCC. The HPLC apparatus used for LCCC experiments consists of a solvent delivery pump (LDC, CM 3200), a six-port sample injector (Rheodyne, 7125), and a variable wavelength UV/vis absorption detector (TSP, Spectra 100). Four C18 bonded silica columns of different pore sizes (Nucleosil C18; 10, 30, 50, 100 nm diameter pore; 250 × 4.6 mm) were used. The column was put in a jacket connected with a bath/circulator to keep the column temperature constant. The mobile phase was a mixture of CH_2Cl_2/CH_3CN (57/43, v/v), and the flow rate was 0.5 mL/min.

For the porosimetry of each column, the column temperature was kept at 40 °C in a column oven, and the eluent was pure CH_2Cl_2 at a flow rate of 0.5 mL/min. Linear PS standards of 10 different molecular weights were run to obtain calibration curves for each column. Column void volumes were measured from the retention volume of toluene (~0.05 g/L in CH_2Cl_2).

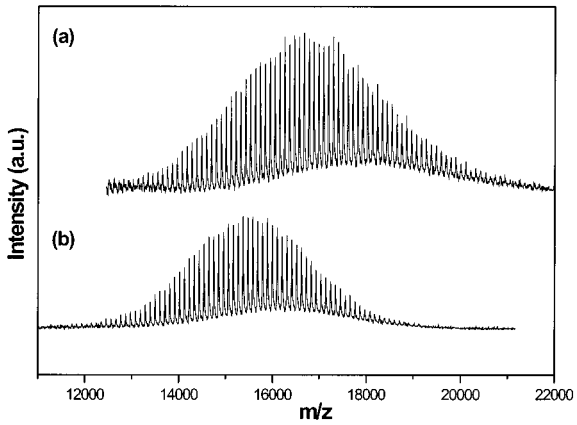

Figure 1. MALDI-TOF MS spectra of linear precursor (a) and of fractionated rings (b) for the sample R16.

Results and Discussion

SEC and MALDI-TOF MS Characterization of Ring PS. Figure 1 shows the MALDI-TOF mass spectrum of the linear precursor (a) and the ring polymer (b) of the sample R16. The mass spectrum of the linear precursor does not show a significant amount of subsidiary peaks. The molecular weights of the main peaks are $104.15N$ (N = degree of polymerization) + 2.02, which exactly corresponds to the molecular structure of polystyrene initiated with sodium naphthalide and terminated with an alcohol. In the spectrum of the ring PS, the molecular weight of the main peaks corresponds well to the ring structure, $104.15N + 58.16$ (dimethylsilyl group), which confirms the chemical homogeneity of the ring polymer. Recently, we found from a rigorous structural analysis of R17 that the ring PS contains a trace amount of double ring except for the linear precursor.[19]

The mass spectra of the linear precursors and the fractionated rings show a clear difference in the molecular weight distribution. The fractionated ring polymer has a smaller average molecular weight, and its molecular weight distribution appears narrower. It seems that the fractional precipitation process to purify the ring polymers from their linear precursors would have removed the high molecular weight portion of the ring polymers. Therefore, we remeasured the molecular weight of ring polymers by SEC-MALLS, and they are summarized in Table 1. The calculated results were similar to but systematically smaller than the previous data by Roovers et al.[5,12] They are in better agreement with the molecular weight measured by MALDI-TOF mass spectrometry. The new set of molecular weights shown in Table 1 was used in this study. The polydispersity (M_w/M_n) values were determined by SEC with respect to the linear PS. The real M_w/M_n values must be smaller than that since it contains a finite amount of precursor polymers, and SEC overestimates the polydispersity of such a narrow distribution polymer due to the band broadening effect.[43]

LCCC Experiment of Linear and Ring PS. In this study, four monomeric C18 bonded silica columns of different nominal pore diameters in the range 10−100 nm were employed. A mixture of CH_2Cl_2 and CH_3CN with a volume ratio of 57/43 was chosen as the mobile phase of the LCCC experiments since this composition provided a chromatographic critical condition for linear PS at around the room temperature if the C18 bonded silica stationary phase was employed.[44,45] At this fixed mobile phase composition, we changed the temperature of the column to find a temperature at which all the different molecular weight linear PS standards (molecular weight range: 5.8×10^2−3.9×10^5) would coelute at the same retention time. The critical temperature had to be found for each column separately since it is very sensitive to the change in mobile as well as stationary phase.[46−48]

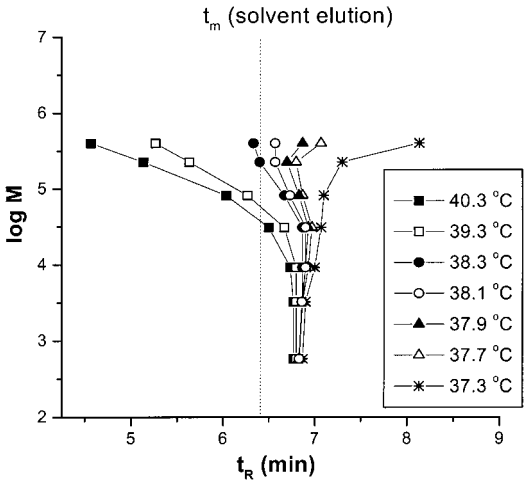

Figure 2. Log (molecular weight) vs retention time plot of linear PSs at various temperatures near the critical condition (10 nm pore column). Flow rate was 0.5 mL/min, and the eluent was a mixture of CH_2Cl_2/CH_3CN (57/43, v/v).

Figure 2 shows a plot of log molecular weight (M) vs retention time (t_R) for linear PS measured with the 10 nm pore size column at various temperatures. As the temperature is decreased from 40.3 to 37.3 °C, the main retention mechanism clearly changes from size exclusion to interaction. However, there does not exist a precise coelution temperature over the entire molecular weight range tested, and a peculiar S-shaped curvature was observed in the vicinity of the critical condition. In Figure 3 are shown the chromatograms of the PS samples obtained at four different temperatures adjacent to the critical temperature. In addition to the S-shaped curvature in the retention time, broadening of the elution peaks becomes distinct as the molecular weight of the sample increases. The similar behavior around the critical condition was previously reported.[46,49−51] At higher molecular weight reliable measurements become practically impossible since even a slightly different solvent composition between the sampling solvent and the mobile phase often causes a distinct peak splitting. It was explained as a manifestation of macroscopic fluctuations between equilibrium and metastable states in the vicinity of the transition point.[52] Although it is hard to unambiguously determine a critical temperature, we chose 37.9 °C as the critical temperature for the 10 nm pore column because the overall departure from the molecular weight independence is the least.

The dotted vertical line in Figure 2 marks the solvent peak position t_m equal to the retention time corresponding to $K = 1$, which is the theoretical prediction for the distribution coefficient of linear macromolecules in the critical point. However, as can be seen in Figure 2, linear polystyrenes at 37.9 °C have higher retention times, which means that $K^{cr} > 1$. The difference $t_R^{cr} - t_m \propto K^{cr} - 1$ becomes smaller with larger pore sized

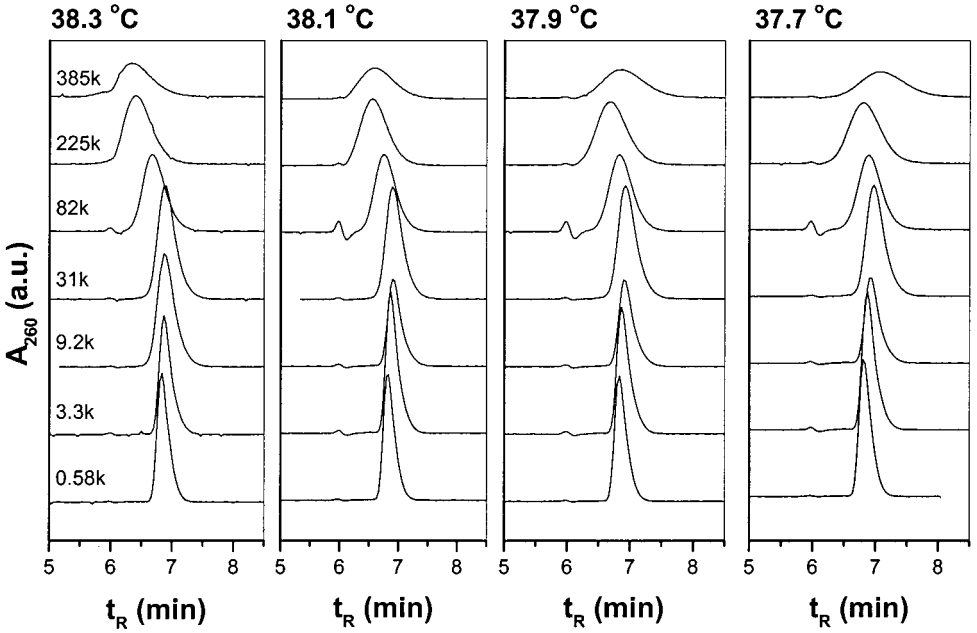

Figure 3. Chromatograms of linear PSs at four different temperatures near the critical condition (10 nm pore column). Flow rate was 0.5 mL/min, and the eluent was a mixture of CH_2Cl_2/CH_3CN (57/43, v/v).

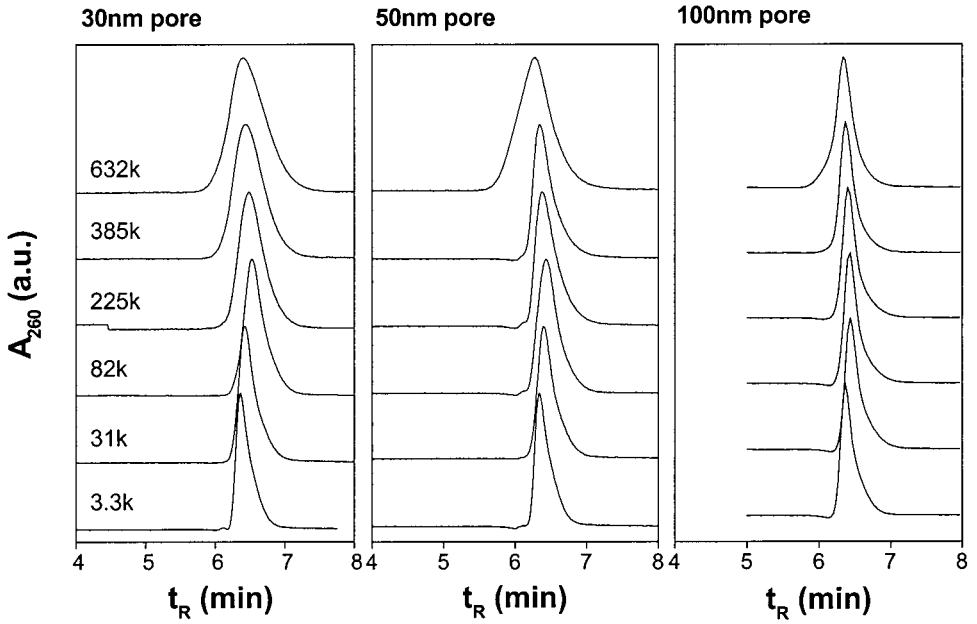

Figure 4. LCCC chromatograms of linear PSs for three columns. From left, 30 nm pore (at 43.1 °C), 50 nm pore (at 41.0 °C), and 100 nm pore column (at 41.5 °C). Flow rate was 0.5 mL/min, and the eluent was a mixture of CH_2Cl_2/CH_3CN (57/43, v/v).

columns, being approximately proportional to $1/d$. Undoubtedly, this effect is due to a contribution of end groups to the enthalpic interaction with stationary phase. Actually, $K^{cr} > 1$ with the pore size dependence of just such type is often observable in studies of functional macromolecules.[32]

When larger pore sized columns are employed, the compensation problem found in 10 nm pore becomes less serious as shown in Figure 4. In these experiments we included an even higher molecular weight PS. It is evident with the 100 nm pore column that coelution temperature can be determined much more unambiguously, and the band broadening is also reduced significantly. The critical temperatures for each pore size column were determined as 43.1 °C (30 nm pore), 41.0 °C (50 nm pore), and 41.5 °C (100 nm pore). There exists a few degrees variation of the critical temperature among the columns, which is seemingly due to the small difference in stationary phase between the columns. It is not significant considering that a large change in critical temperature is observed with a minute variation in the eluent composition.[44,46,47]

At the critical condition for each column, retention times of ring PSs were measured and are listed in Table 2. Results of two independent measurements are shown for 10 and 30 nm columns with which the ambiguity of the critical condition is more serious, which show the repeatability of the measurements is reasonable. We also tested the effect of mobile phase flow rate in order to ensure that the chromatographic separation process is under pseudoequilibrium condition since theories of chromatographic separation are developed under the assumption of an equilibrium distribution. In Figure 5, LCCC chromatograms of ring PSs using 30 nm pore

Table 2. Peak Retention Time of Ring PSs under the Critical Condition of Linear PS

sample code	t_R (min)[a]					
	10 nm pore		30 nm pore			
	first	second	first	second	50 nm pore	100 nm pore
R17	6.95	6.95	6.50	6.57	6.37	6.40
R7	7.50	7.50	6.78	6.88	6.53	6.47
R16	7.75	7.73	6.92	7.02	6.63	6.47
R1	7.95	7.89	7.05	7.16	6.67	6.53
R4	8.50	8.40	7.57	7.62	6.97	6.67
R8	8.65	8.50	7.80	7.86	7.12	6.73
R9	8.70	8.50	7.87	7.94	7.15	6.73
R18	8.45	8.11	8.20	8.17	7.37	6.93
R10	8.20	7.81	8.22	8.17	7.45	6.93

[a] Flow rate was 0.5 mL/min.

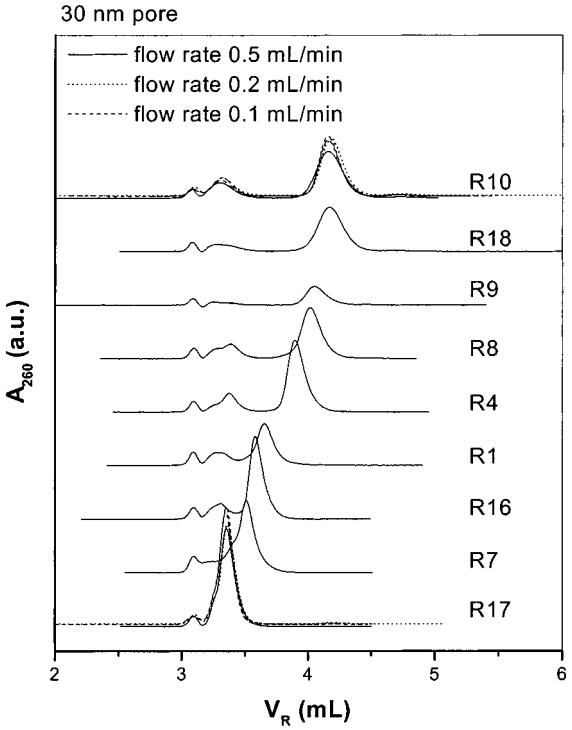

Figure 5. LCCC chromatograms of ring PSs (30 nm pore column). For R10 and R17, chromatograms obtained at three different flow rates are shown.

column taken at three different flow rates are displayed. As clearly shown in the figure, the sample retention volumes and peak shapes remain practically unchanged down to the flow rate of 0.1 mL/min, confirming the retention volume is independent of the flow rate. The small peak near $V_R = 3.1$ mL is the injection solvent peak, and the linear precursors left in the fractionated ring PS samples are eluted near $V_R = 3.3$ mL. The retention volume of ring PS increases with molecular weight under the critical condition of linear PS. As previously reported,[16] the trend of the ring PSs' retention with respect to the molecular weight is in good qualitative agreement with the theoretical prediction by Gorbunov and Skvortsov.[38]

Porosimetry of Columns. To compare the experimental results with the existing theory, we first need to determine the parameter Σ for the columns used. It was established that the inverse SEC method is a direct method of the determination of the parameter Σ. According to the SEC theory developed by Casassa[36] for models of different pore shapes, the slope of the dependence of K_{SEC} on R at small R regime is simply proportional to Σ.[40]

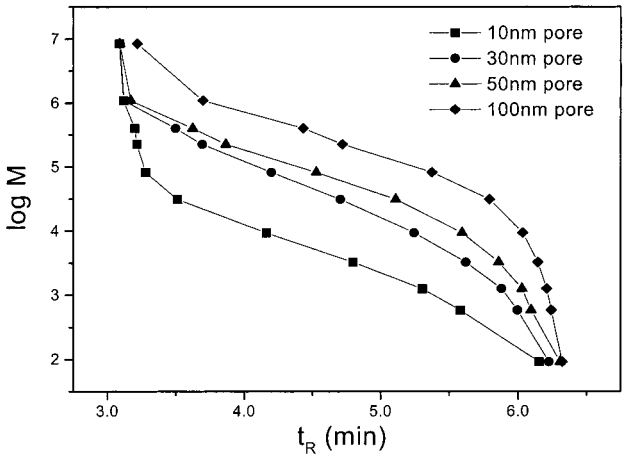

Figure 6. Log (molecular weight) vs retention time plot of linear PSs at SEC condition for four columns of different pore sizes. Flow rate was 0.5 mL/min, and the eluent was CH_2Cl_2.

$$K_{SEC} \approx 1 - \frac{2p}{\sqrt{\pi}}\frac{R}{d} = 1 - \frac{2}{\sqrt{\pi}} R\Sigma \qquad (12)$$

where $p = 1$, 2, and 3 for slitlike, cylindrical, and spherical pores.

The pore size distribution also can be determined by the inverse SEC method. The inverse SEC method is based on the formula (in this formula the pore transverse dimension $D = 2d$ is used in order to avoid the confusion of the pore size d with the differential symbol):

$$K_{SEC}(R) = \int_0^\infty K\left(\frac{R}{D}\right)\varphi(D)\, dD \qquad (13)$$

where $K(R/D)$ is the full theoretical function taken from the SEC theory of Casassa, and $\varphi(D)$ is the pore size distribution (PSD) function. Having the experimentally obtained function $K_{SEC}(R)$ and the theoretical kernel function, $K(R/D)$, $\varphi(D)$ can be obtained from the best fit of the experimental points to the calculated curve. To make these calculations, we used a software described in the previous paper,[40] which is available now as PSS POROCheck software from Polymer Standards Service GmbH (Mainz). The radius of gyration of polystyrene in a good solvent, R, was calculated by using the following equation measured by neutron scattering in deuterated toluene.[9]

$$R\ (\text{nm}) = 0.012285 M^{0.5947} \qquad (14)$$

In Figure 6, SEC retention data of PS samples in CH_2Cl_2 are shown in the form of SEC calibration curves. Using these data, the distribution coefficient, K_{SEC}, was calculated according to the following equation:

$$K_{SEC} = \frac{V_r - V_0}{V_p} \qquad (15)$$

$V_0 + V_p$ and V_0 (limits of total permeation and total exclusion, respectively) values were taken from the retention volumes of toluene and 8410 kg/mol molecular weight PS, respectively.

Figure 7 shows K_{SEC} vs R dependencies of the four columns. Points are the data calculated by eq 15 from the experimental retention data shown in Figure 6, and

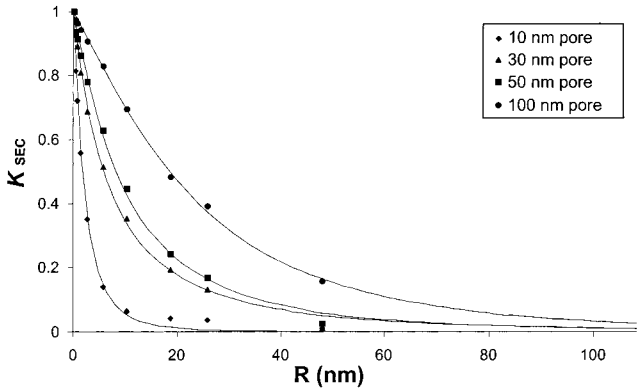

Figure 7. K_{SEC} vs radius of the PS plot for four columns of different pore sizes. Different symbols are the retention data shown in Figure 6, and the solid lines are the best fit to eq 13.

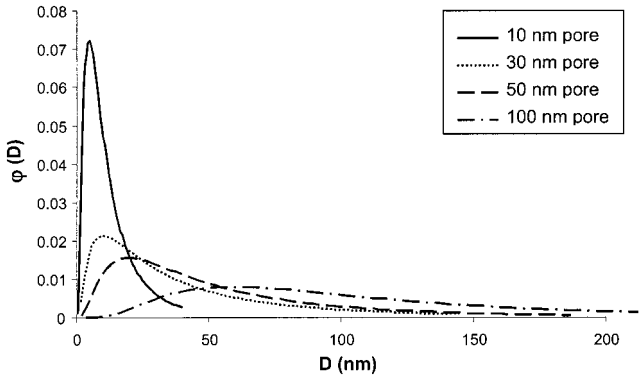

Figure 8. Pore size distribution of the four columns obtained from the fit shown in Figure 7 according to eq 13.

Table 3. Results of Porosimetry

nominal pore diameter (nm)	$\Sigma = S_p/V_p$ (m^2/cm^3)	$\langle D\rangle$ (nm)	$\sigma/\langle D\rangle$
10	304 ± 20	6.6 ± 0.4	1.01 ± 0.12
30	113 ± 9	17.7 ± 1.4	1.45 ± 0.15
50	69 ± 6	28.9 ± 2.4	1.09 ± 0.15
100	27 ± 1	74 ± 3	0.75 ± 0.07

lines are the best fit to eq 13. The pore size distribution functions, $\varphi(D)$, obtained in the result of this fitting procedure are shown in Figure 8, and the main porosimetric results are summarized in Table 3. $\langle D\rangle$ is the average width of equivalent slitlike pores. (The diameter of equivalent cylindrical pores is 2 times larger.) The mathematical definition of $\langle D\rangle$ is the following:

$$\langle D\rangle = p\frac{V_p}{S_p} = [\int_0^\infty D^{-1}\varphi(D)\,dD]^{-1} \qquad (16)$$

The parameter related to the width of the PSD function is presented in the last column. Here σ is the square root of the dispersion of the pore size distribution function. Since we need only the parameter Σ in the present study, we shall not discuss the PSD function further except that for all four columns the average pore size $\langle D\rangle$ is close to two-thirds of the nominal pore size and the pore size distribution is quite broad.

The confidence intervals denoted in Table 3 correspond to the scattering of experimental points around the calculated curves in Figure 7. These intervals do not include the possible errors related to the values of R that were used in the calculation. To estimate these possible errors, we used the different formula for R of

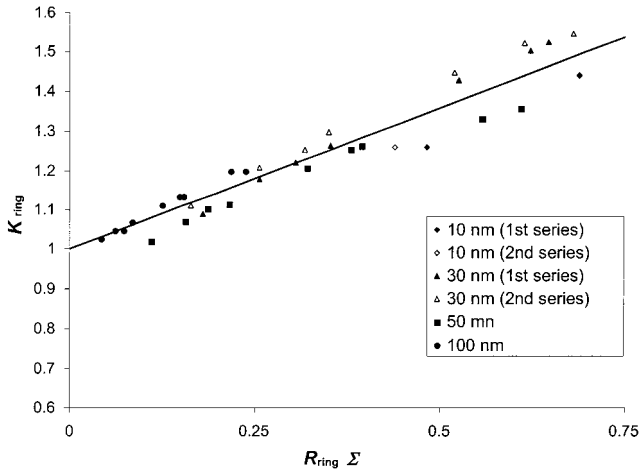

Figure 9. Critical condition distribution coefficient of ring PS vs $R_{ring}\Sigma$ at $R_{ring}\Sigma < 0.7$. Straight line is a linear approximation.

polystyrenes in another good solvent (THF, 25 °C).[53]

$$R\,(\text{nm}) = 0.0139M^{0.588} \qquad (17)$$

The values of Σ obtained with use of the inverse SEC method and PS radii calculated from eq 17 are 283, 105, 65, and 27 m^2/cm^3 for the columns denoted as 10, 30, 50, and 100 nm, respectively. These values are lower than those presented in Table 3, but the difference is rather small, less than 8%.

Comparison between Experimental Results and Theoretical Prediction; Wide Pore Behavior. Let us recall the theoretical result obtained for the distribution coefficient of the ideal ring macromolecules in the case of critical adsorption point and wide pores:

$$K_{ring} \approx 1 + \sqrt{\frac{\pi}{2}}R_{ring}\Sigma \qquad (18)$$

To compare the experimental data with eq 18, we plotted the distribution coefficient, K_{ring}, as a function of a parameter $R_{ring}\Sigma$. (For a slitlike pore this parameter is equal to R_{ring}/d.) However, it was practically impossible to perform direct measurements of the radius of gyration (R_g) of ring polystyrenes in the critical solvent condition due to the limited amount of the ring polymer samples and their relatively low molecular weight. Therefore, instead of R_g the hydrodynamic radius, R_h (that is the equivalent Stokes radius), measured by dynamic light scattering technique was used in the calculation.[54] We obtained the following equation for R_h of ring polystyrenes in our mixed-solvent eluent system as a function of molecular weight:

$$R_{h,ring}\,(\text{nm}) = 0.02111M^{0.4989} \qquad (19)$$

We first focus our attention on the $R_{ring}\Sigma \ll 1$ case, for which eq 18 is applicable. To prepare Figure 9 only the data corresponding to $R_{ring}\Sigma < 0.7$ were selected.

As shown in Figure 9, the experimental data plotted in the coordinates of $R_{ring}\Sigma$ undoubtedly form a universal dependence. This experimental fact is in good qualitative agreement with the theoretical formula, eq 18. Moreover, in full accordance with the theory, this dependence can be approximated by a linear function. The approximate experimental formula obtained for

system under investigation in the wide-pore limit can thus be written in the form:

$$K_{ring} \approx 1 + 0.718 R_{h,ring} \Sigma \qquad (20)$$

Interestingly, the coefficient in the experimental formula (20) significantly differs from the predicted coefficient in eq 18, $\sqrt{\pi/2} \approx 1.253$.

Although we cannot fully account for this discrepancy, we can consider a few points to explain the deviation in the slope from the theoretical prediction as follows:

(1) Deviation from the true critical condition: As follows from the theory, the results at $R/d \ll 1$ should not be very sensitive to possible deviations of the system from the adsorption transition point.[38,55]

(2) Using R_h instead of R_g: It is well-known that R_g is larger than R_h. Therefore, using R_g is going to stretch the abscissa of Figure 9, which would make the deviation even larger.

(3) Using slitlike pore geometry: The pores of the columns used must have a complicated geometry that cannot be assumed simply as slitlike or cylinder.[56] However, the final result in the limit of $R/d \ll 1$ contains only one parameter related to the porous structure, namely the parameter $\Sigma = S_p/V_p$ (the ratio of the pore surface area to the pore volume) although the theory[55] was developed for the model of slitlike pores (of width $2d$). The definition of this parameter does not require any special model for the pores, and this parameter has a meaning even for pores of irregular shape. Because of the same argument, we also expect that possible pore size distribution will not much influence the results at $R/d \ll 1$. (In fact, it was proven theoretically, again for the model of slitlike pores, that in the case of pore size distribution the result at $R/d \ll 1$ is expressible in terms of $1/\Sigma$.)

(4) R_g values in *d*-toluene used in the porosimetry calculation: The solvent (eluent) was CH_2Cl_2 in the inverse SEC porosimetry while a mixed solvent was used for LCCC measurements. Since both toluene and CH_2Cl_2 are known to be good solvents for PS, there would not be much difference in R_g in two solvents. Therefore, pore size measurements of the columns in good solvent condition should not be a significant source of errors. However, the difference of the solvent in inverse SEC porosimetry and LCCC can be significant since the nature of the solvent might have affected the surface area and the pore diameter of the column. Unfortunately we do not have other choices since the inverse SEC method requires a good solvent eluent in order to ensure the separation by the size exclusion mechanism.

(5) A question related to the ideal-chain model used as a background for our porosimetric method and also in the critical condition theory: We applied this model to describe the chromatographic behavior of the real macromolecules in different solvents, so one may think that the coefficients $2/\sqrt{\pi}$ in eq 12 and $\sqrt{\pi}/2$ in eq 6 can be different for our real systems. For linear polymers in SEC conditions, this question has been already discussed by Casassa,[36] and the conclusion was that eq 12 can be also used for the good solvents. The coefficient $\sqrt{\pi}/2$ of eq 6, related to the span of a ring chain, appears also in the SEC theory for ring macromolecules,[35] which happened to be in a very good quantitative agreement with SEC experiments in a good solvent. Furthermore, the critical mixed eluent system is close to the Θ condition since the molecular weight exponent of the diffusivity determined by dynamic light scattering was very close to 0.5 (eq 19).

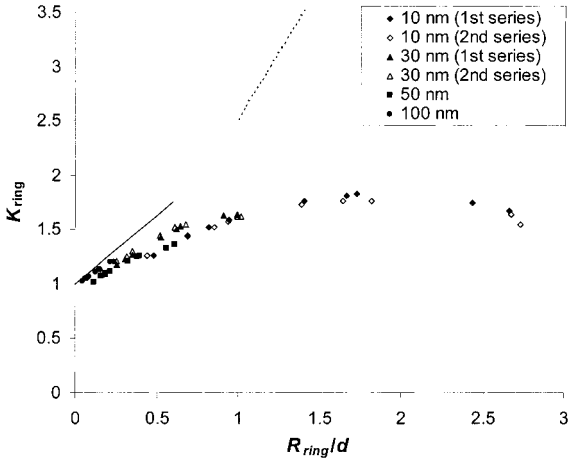

Figure 10. Critical condition distribution coefficient of ring PS in the whole measured range of molecule-to-pore size ratio. The experimental data are marked by symbols; solid and dotted lines correspond to eqs 6 and 7 for low and high R/d.

Experimental Results and Theoretical Predictions for Narrow-Pore Regime. Now let us turn to the behavior of ring polymers in narrow pores. Figure 10 shows a plot of K_{ring} vs R_{ring}/d for the whole studied range of R_{ring}/d. (To plot the experimental data, we again used as R_{ring} the hydrodynamic radius R_h of ring polystyrenes, calculated from eq 19, instead of the radius of gyration R_g.) The discrepancy between the experimental result at $R_{ring}/d \gg 1$ and the ideal-chain theory is clearly seen in Figure 10. Unlike the prediction of the theory (eq 7), the experimental points form a nonmonotonic curve with a downward curvature at $R_{ring}/d \gg 1$. Similar nonmonotonic behavior of the distribution coefficient of ring macromolecules in the critical conditions has also been observed previously by Blagodatskikh and Gorshkov.[28]

It is obvious that the ideal-chain theory is not able to explain this experimental result; therefore, we shall also try to find an explanation in the framework of the scaling approach, which takes into account of excluded volume effects.

(1) Possible influence of the solvent quality and pore dimensionality: Since our solvent was quite close to the Θ solvent, we may substitute into eq 11 the indices $\nu_3 = {}^1/_2$, $\nu_2 = {}^2/_3$, and $\nu_1 = 1$ for three-, two-, and one-dimensional cases for a polymer chain in the Θ solvent.[38] This will give us the following adsorption transition point indices for the ring macromolecules; $\delta_{ring} = 1$ in the case of $f = 1$ (cylindrical pores) and smaller, but still positive value of $\delta_{ring} = {}^1/_3$ for $f = 2$ (slitlike pores). Therefore, both solvent quality and pore dimensionality cannot make K_{ring} be a decreasing function of R/d.

(2) Possible nonequivalence in the conditions for theory and experiment: In the experiment we searched the critical condition as a point, at which K is independent of molecular weight in the whole range of M. It was already mentioned that at $R/d > 1$ there was no exact independence of K on M, and therefore there was an ambiguity in our choice, especially in the case of 10 nm column. We also discussed a difference in the conditions for the ideal-chain and the scaling theories. Both theories were, in fact, developed for the exclusion−

adsorption transition point. For the ideal-chain theory of linear macromolecules the transition point was proved to be the same as the point of independence of K of M. However, this occurred to be not the case for linear polymers with the excluded volume; the scaling theory generally does not give the independence of K on molecular weight in the transition point. Moreover, the scaling theory predicted the impossibility to find a point of exact molecular weight independence for linear polymers with excluded volume in the case of $R/d \gg 1$. Monte Carlo simulation of linear polymer chains with the excluded volume,[51] recent experimental observations,[46,48−50] and the results of the present study (Figures 2 and 3) seem to support this fact. Because of the ambiguity in the definition of the critical condition, it is quite likely that the condition for the narrow-pore column was not exactly equivalent to that of the discussed theories, namely that the experimentally realized interaction was weaker than the exclusion−adsorption transition point interaction. If this is really the case, then the observed retention behavior of ring polystyrenes at high R/d must be compared with a more general theory of chromatography of polymers,[38] which accounts also for a deviation from the transition point. Since at weaker interactions this more general theory predicts for ring macromolecules just such nonmonotonic dependence of K on M, as observed in the present study, the deviation of the experimental condition from the true adsorption transition point seems to be a quite possible explanation of the observed chromatographic behavior of ring polystyrenes at $R/d \gg 1$.

(3) Detailed pore structure: Apart from the above-discussed factors of the pore dimensionality and the excluded volume, the details of the in-pore space topology may also be of importance. For example, it is well-known that ring polymers of high molecular weights in the network of fixed topological constraints or obstacles take conformations, which are similar to those of branched polymer chain[57,58]—the lattice equivalents of these conformations are often called "lattice animals".[59] Such in-pore topological constraints were not taken into account in the theories discussed above, and the influence of these topological factors on the chromatographic behavior of ring macromolecules has not been studied yet. The nonhomogeneity in pore size and shape, which has not been accounted for, may also be of importance in the case of $R/d \gg 1$.

(4) Chemical difference of ring PS and linear PS: The LCCC behavior of linear polystyrenes revealed that the presence of specific end groups affects the retention significantly, which has been utilized for the characterization of telechelic polymers.[32] Ring PS contains a dimethylsilyl linking group in a chain which could influence the critical behavior of the polymers. However, since there are no systematic shifts between the data series in Figures 9 and 10, the linking group does not seem to alter the LCCC retention of ring PS significantly.

Irrespective of whether our experimental condition was the true point of the adsorption phase transition, the observed chromatographic condition has proved to provide for a very effective separation of polydisperse ring and linear polystyrenes. To investigate the mechanism of this separation in more detail and to explain more clearly the observed chromatographic behavior of ring polystyrenes, it would be interesting to extend the experimental study in order to cover different temperatures or mobile phase compositions around the critical point and to consider the experimental results together with the more general theory, which accounts for arbitrary adsorption interaction. Monte Carlo simulations of ring macromolecules with the excluded volume in narrow pores of different geometry, similar to those reported by Cifra and Bleha for linear polymers,[51] could also bring additional insight into the mechanism of chromatography of ring polymers.

Summary

We performed a detailed investigation of the retention of ring polystyrenes at the chromatographic condition, which was estimated as being close to the critical condition for linear PS. Reversed phase columns of various pore size were examined. Assuming slitlike pore geometry, the porosimetry of every column was performed following the calculation of the distribution coefficient of cyclic polystyrenes near the critical condition of linear PS. Within a wide pore regime ($R_{ring}/d \ll 1$), the calculated distribution coefficient of ring PS showed a nice universal dependence regardless of column pore size as predicted by theory. However, the slope of the plot was not in quantitative agreement with the theory. Significant deviations from the ideal-chain theory were observed in the narrow pore regime ($R_{ring}/d > 1$). We considered a few possible reasons to take into account of these deviations including possible differences in the conditions for theory and experiment.

A new more general definition of the critical condition is introduced in this paper, in which the critical condition is defined as a point of the adsorption phase transition. This new critical point definition is theoretically consistent for both linear and ring polymers as well as for both ideal-chain and excluded-volume macromolecules. The previously reported experimental observations and Monte Carlo simulation results also seem to support the general definition of the critical condition.

Acknowledgment. T.C. acknowledges the supports from KRF (BK21 program) and KOSEF (Center for Integrated Molecular Systems).

References and Notes

(1) Naghizadeh, J.; Sotobayashi, A. *J. Chem. Phys.* **1974**, *60*, 3104.
(2) Baumgartner, W. *J. Chem. Phys.* **1982**, *76*, 4275.
(3) Garcia Bernal, J. M.; Tirado, J. J.; Freire, M. M.; Garcia de la Torre, J. *Macromolecules* **1990**, *23*, 3357.
(4) Vollmert, B.; Huang, J. X. *Makromol. Chem. Rapid Commun.* **1981**, *2*, 467.
(5) Roovers, J. *J. Polym. Sci., Part B* **1985**, *23*, 1117.
(6) Lutz, P.; Mckenna, G. B.; Rempp, P.; Strazielle, C. *Makromol. Chem. Rapid Commun.* **1986**, *7*, 599.
(7) McKenna, G. B.; Hadziioannou, G.; Lutz, P. *Macromolecules* **1987**, *20*, 498.
(8) Higgins, J. S.; Dodgson, K.; Semlyen, A. *Polymer* **1979**, *20*, 553.
(9) Ragnetti, M.; Geiser, D.; Hocker, H.; Oberthur, R. C. *Makromol. Chem.* **1985**, *186*, 1701.
(10) Hadziioannou, G.; Cotts, P. M.; ten Brinke, G.; Han, C. C.; Lutz, P.; Strazielle, C.; Rempp, P.; Kovacs, A. J. *Macromolecules* **1987**, *20*, 493.
(11) Duval, M.; Lutz, P.; Strazille, C. *Makromol. Chem. Rapid Commun.* **1985**, *6*, 71.
(12) Roovers, J. *Macromolecules* **1985**, *18*, 1359.
(13) Roovers, J. *Macromolecules* **1988**, *21*, 1517.
(14) Roovers, J.; Toporowski, P. M. *J. Polym. Sci., Part B* **1988**, *26*, 1251.
(15) Pasch, H.; Deffieux, A.; Henze, I.; Schappacher, M.; Rique-Lurbet, L. *Macromolecules* **1996**, *29*, 8776.

(16) Lee, H. C.; Lee, H.; Lee, W.; Chang, T. *Macromolecules* **2000**, *33*, 8119.
(17) Lepoittevin, B.; Dourges, M. A.; Masure, M.; Hemery, P.; Baran, K.; Cramail, H. *Macromolecules* **2000**, *33*, 8218.
(18) Pasch, H.; Deffeux, A.; Ghahary, R.; Schapacher, M.; Rique-Lurbet, L. *Macromolecules* **1997**, *30*, 98.
(19) Cho, D.; Park, S.; Kwon, K.; Chang, T. *Macromolecules* **2001**, *34*, 7570.
(20) Hild, G.; Kohler, A.; Rempp, P. *Eur. Polym. J.* **1980**, *16*, 525.
(21) Vollmert, B.; Huang, J. X. *Mackromol. Chem., Rapid Commun.* **1980**, *1*, 333.
(22) Geiser, D.; Hocker, H. *Macromolecules* **1980**, *13*, 653.
(23) Roovers, J.; Toporowski, P. M. *Macromolecules* **1983**, *16*, 843.
(24) Dodgson, K.; Semlyen, J. A. *Polymer* **1977**, *18*, 1265.
(25) Yu, G. E.; Sun, T.; Yan, Z. G.; Price, C.; Booth, C.; Cook, J.; Ryant, A. J.; Viras, K. *Polymer* **1997**, *38*, 35.
(26) Dodgson, K.; Sympson, D.; Semlyen, J. A. *Polymer* **1978**, *19*, 1285.
(27) Dagger, A. C.; Semlyen, J. A. *Polymer* **1999**, *40*, 3243.
(28) Blagodatskikh, I. V.; Gorshkov, A. V. *Vysokomol. Soedin. Ser. A* **1997**, *39*, 1681.
(29) Belenki, B. G.; Gankina, E. S.; Tennikov, M. B.; Vilenchik, L. Z. *Dokl. Akad. Nauk. SSSR* **1976**, *231*, 1147.
(30) Gorshkov, A. V.; Much, H.; Becker, H.; Pasch, H.; Evreinov, V. V.; Entelis, S. G. *J. Chromatogr.* **1990**, *523*, 91.
(31) Zimina, T. M.; Kever, J. J.; Melenavskaya, E. Y.; Fell, A. F. *J. Chromatogr.* **1992**, *593*, 233.
(32) Pasch, H.; Trathingg, B. *HPLC of Polymers*; Springer-Verlag: Berlin, 1998.
(33) Lee, H.; Lee, W.; Chang, T.; Choi, S.; Lee, D.; Ji, H.; Nonidez, W. K.; Mays, J. W. *Macromolecules* **1999**, *32*, 4143.
(34) Berek, D.; Janco, M.; Hatada, K.; Kitayama, T.; Fujimoto, N. *Polym. J.* **1997**, *29*, 1029.
(35) Gorbunov, A. A.; Skvortsov, A. M. *Vysokomol. Soedin* **1984**, *26A*, 2062.
(36) Casassa, E. F. *J. Polym. Sci., Part B* **1967**, *5*, 773.
(37) de Gennes, P. G. *J. Polym. Sci., Part B* **1969**, *5*, 773.
(38) Gorbunov, A. A.; Skvortsov, A. M. *Adv. Colloid Interface Sci.* **1995**, *62*, 31.
(39) Casassa, E. F. *Macromolecules* **1976**, *9*, 182.
(40) Gorbunov, A. A.; Solovyova, L. Y.; Pasechnik, V. A. *J. Chromatogr.* **1988**, *448*, 307.
(41) Skvortsov, A. M.; Gorbonov, A. A. *Vysokomol. Soedin., Ser. A* **1986**, *28*, 1686.
(42) de Gennes, P. G. *Scaling Concepts in Polymer Physics*; Cornell University Press: Ithaca, NY, 1979.
(43) Lee, W.; Lee, H.; Cha, J.; Chang, T.; Hanley, K. J.; Lodge, T. P. *Macromolecules* **2000**, *33*, 5111.
(44) Chang, T.; Lee, W.; Lee, H. C.; Park, S.; Ko, C. *Macromol. Chem. Phys.* **1999**, *200*, 2188.
(45) Lee, W.; Cho, D.; Chun, B. O.; Chang, T.; Ree, M. *J. Chromatogr. A* **2001**, *910*, 51.
(46) Philipsen, H. J. A.; Klumperman, B.; van Herk, A. M.; German, A. L. *J. Chromatogr. A* **1996**, *727*, 13.
(47) Lee, W.; Cho, D. H.; Chang, T.; Hanley, K. J.; Lodge, T. P. *Macromolecules* **2001**, *34*, 2353.
(48) Lee, W.; Park, S.; Chang, T. *Anal. Chem.* **2001**, *73*, 3884.
(49) Berek, D.; Janco, M.; Meira, G. R. *J. Polym. Sci., Part A: Polym. Chem.* **1998**, *36*, 1363.
(50) Baran, K.; Laugier, S.; Cramail, H. *Macromol. Chem. Phys.* **1999**, *200*, 2074.
(51) Cifra, P.; Bleha, T. *Polymer* **2000**, *41*, 1003.
(52) Brun, Y. *J. Liq. Chromatogr. Relat. Technol.* **1999**, *22*, 3067.
(53) Knox, J. H.; Scott, H. P. *J. Chromatogr.* **1984**, *318*, 311.
(54) Lee, H.; Chang, T.; Roovers, J., unpublished results.
(55) Gorbunov, A. A.; Skvortsov, A. M. *Vysokomol. Soedin., Ser. A* **1987**, *29*, 1025.
(56) Snyder, L. R.; Kirkland, J. J. Introduction to Modern Liquid Chromatography; Wiley-Interscience: New York, 1979; p 168.
(57) Khokhlov, A. R.; Nechaev, S. K. *Phys. Lett. A* **1985**, *112*, 156.
(58) Obukhov, S. P.; Rubinstein, M.; Duke, T. *Phys. Rev. Lett.* **1994**, *73*, 1263.
(59) Muller, M.; Wittmer, J. P.; Cates, M. E. *Phys. Rev. E* **2000**, *61*, 4078.

MA0109222